

Spiral Waves in Chaotic Systems

Andrei Goryachev and Raymond Kapral
Chemical Physics Theory Group, Department of Chemistry,
University of Toronto, Toronto, ON M5S 1A1, Canada

Spiral waves are investigated in chemical systems whose underlying spatially-homogeneous dynamics is governed by a deterministic chaotic attractor. We show how the local periodic behavior in the vicinity of a spiral defect is transformed to chaotic dynamics far from the defect. The transformation occurs by a type of period doubling as the distance from the defect increases. The change in character of the dynamics is described in terms of the phase space flow on closed curves surrounding the defect.

Spiral waves are commonly observed in oscillatory and excitable media. [1] They are often responsible for the patterns one sees in chemical systems and can give rise to spatiotemporal states such as defect-mediated turbulence whose erratic dynamics is characterized by the creation and destruction of pairs of defects (spiral wave cores) with opposite topological charge. [2] The topological charge n_t is defined by [3]

$$\frac{1}{2\pi} \oint \nabla \phi(\mathbf{r}) \cdot d\mathbf{l} = n_t, \quad (1)$$

where $\phi(\mathbf{r})$ is the local phase and the integral is taken along a closed curve surrounding the defect.

In this article we examine the nature of such spiral wave states in chemical media where the underlying dynamics is itself chaotic. More specifically, we consider systems where the dynamics of the spatially homogeneous system, described by ordinary differential equations, has a deterministic chaotic attractor which arises through a period-doubling cascade. Consequently, the simplest models for the dynamics considered here require at least three phase space variables in contrast to the two-variable descriptions of excitable or oscillatory media. [1] We examine how this local deterministic chaos can support spiral waves in the spatially-distributed medium. We also show that systems of this kind can exhibit defect-mediated turbulence and demonstrate that the underlying local temporal dynamics is quite different from that in simple oscillatory media.

Consider the Willamowski-Rössler [4] reaction-diffusion equations,

$$\begin{aligned} \frac{\partial c_x(\mathbf{r}, t)}{\partial t} &= \kappa_1 c_x - \kappa_{-1} c_x^2 - \kappa_2 c_x c_y + \kappa_{-2} c_y^2 - \kappa_4 c_x c_z + \kappa_{-4} + D \nabla^2 c_x, \\ \frac{\partial c_y(\mathbf{r}, t)}{\partial t} &= \kappa_2 c_x c_y - \kappa_{-2} c_y^2 - \kappa_3 c_y + \kappa_{-3} + D \nabla^2 c_y, \\ \frac{\partial c_z(\mathbf{r}, t)}{\partial t} &= -\kappa_4 c_x c_z + \kappa_{-4} + \kappa_5 c_z - \kappa_{-5} c_z^2 + D \nabla^2 c_z, \end{aligned} \quad (2)$$

where $c_\tau(\mathbf{r}, t)$ is the local concentration of species $\tau = x, y, z$ (we have suppressed the arguments of c_τ on the right hand side of (2)) and $\kappa_{\pm i}$ are rate coefficients that contain the concentrations of species that are fixed to maintain the system out of equilibrium. The diffusion coefficients of all three species are equal to D .

Suppose the system is spatially homogeneous and the dynamics is described by the ordinary differential equations based on the reactive terms in (2). The resulting mass action rate law supports a chaotic attractor that arises by a period-doubling cascade. [4,5] The chaotic attractor in the (c_x, c_y, c_z) phase space is oriented so that its projection onto the (c_x, c_y) plane clearly exhibits the (folded) phase space flow around the unstable fixed point (focus) $\mathbf{c}^* = (c_x^*, c_y^*, c_z^*)$ which spawned the attractor. Consequently, to define the phase angle ϕ we change variables from $\mathbf{c} = (c_x, c_y, c_z)$ to a cylindrical coordinate system (ρ, ϕ, z) with origin at \mathbf{c}^* and z directed along c_z . [6] As the system undergoes a sequence of period-doubling bifurcations ϕ increases by $2\pi 2^n$ with each period of the

oscillation, where 2^n , $n = 1, 2, 3 \dots \infty$, is the periodicity of the attractor. For period-1 oscillations the other two variables can be uniquely parametrized by the phase ϕ , $\rho = \rho(\phi)$, $z = z(\phi)$ but this is no longer true after the first period doubling bifurcation. However, this variable suffices for the determination of the location and charge of a topological defect in the spatially-distributed medium.

Next we consider the spatially-distributed chaotic system. Figure 1 is a plot of the local phase angle $\phi(\mathbf{r})$ in a two-dimensional medium obtained by numerically integrating (2). [7] One sees a complex pattern of spiral defects whose number varies with time. All defects have topological charge $n_t = \pm 1$. The system evolved from an initial state with a single defect in the center of the system [8]. In the early stages of the evolution the overall number of defects grows rapidly and then, depending on the ratio of the diffusion length to the system size, it either saturates monotonously or rises to a maximum and decreases to some stationary average value about which it fluctuates. Note the different rates of evolution in certain parts of the medium. While the dynamics has an almost periodic character in the regions subject to the organizing influence of large, well-established spirals (upper left and lower right corners of the panels) the evolution is much faster in domains where vortex-antivortex birth and annihilation take place (the vortex-antivortex pair seen in the lower left corners of the first two panels disappears as time increases). From visual inspection of the individual snapshots of the local phase in this figure it is difficult to detect differences between this type of defect-mediated turbulence and that in oscillatory media. Nevertheless, fundamentally different kinds of local dynamics consisting of perturbed period-doubled cycles and chaotic motion underlie and influence the dynamics of the spiral structures seen in this figure.

The very fact that stable spiral waves exist in a medium with underlying chaotic dynamics demonstrates that the reaction-diffusion kinetics in the vicinity of the spiral centers is by no means chaotic – the spiral dynamics locally suppresses the chaos. [9] However, the behavior in those parts of the medium which are sufficiently far from any topological defect shows neither temporal nor spatial order.

Thus, we must consider how the local, period-1, spatio-temporal dynamics near a defect is transformed into complex chaotic dynamics far from a defect. For this purpose we now examine the local dynamics in a reference frame that is centered on one of the defects. We denote the time-dependent position of a defect in the xy plane as $\mathbf{r}_d(t)$ and work in a polar coordinate system (r, θ) centered on $\mathbf{r}_d(t)$. The local concentration fields may now be expressed in these coordinates: $\mathbf{c}(r, \theta, t)$. To investigate this local dynamics in detail we choose the diffusion coefficient to be sufficiently large and use no-flux boundary conditions so that the medium supports a single spiral wave that persists for long periods of time. Panels (a)-(c) of Fig. 2 show trajectories in the concentration phase space, $\mathbf{c}(r, \theta, t)$, for several values of r along a ray emanating from the defect oriented at an angle $\theta = 3/4\pi$. One observes a period-doubling progression from a perturbed period-1 limit cycle near the defect, to perturbed period-2 and period-4 attractors as the distance increases. [10] This basic pattern of period doublings is observed for all angles but the circular symmetry of the system is not maintained. The origin of this effect will be discussed below when the dynamics on closed paths surrounding the defect is examined.

Variants of this phenomenon were seen in the defect-mediated turbulent regime when the dynamics was observed in a coordinate frame centered on a moving defect. Far enough from the defect, locally one finds chaotic dynamics (cf. Fig. 2 (d)) which is suppressed in the vicinity of the defect. Viewed from the defect, as r increases, chaos appears by a truncated period-doubling cascade, similar to that seen in stochastically perturbed versions of flows and maps with no spatial degrees of freedom. [11] We are now faced with the question of how the locally periodic dynamics can transform to locally chaotic dynamics as r varies and maintain the spiral wave structure in the vicinity of the spiral core.

The nature of this transformation can be deduced from the temporal behavior of $\mathbf{c}(r, \theta, t)$ for some fixed value of r , say r' . Suppose the defect has $n_t = +1$ so that the phase ϕ must change by 2π as θ varies through 2π and r' is such that the local dynamics at (r', θ) is a period- 2^n attractor. Thus, even though the phase space trajectory of an individual point on the circle with radius r' may be a period- 2^n attractor, the set of points $\mathcal{S} = \{\mathbf{c}(r, \theta, t) : 0 \leq \theta \leq 2\pi, r = r', t = t_1\}$ must form a closed curve $\mathcal{S} = \mathcal{S}(\mathbf{c})$ which loops once around \mathbf{c}^* in the \mathbf{c} phase space. The curve

\mathcal{S} cannot span the period- 2^n attractor which loops \mathbf{c}^* 2^n times in the course of a cycle. However, \mathcal{S} deforms as time evolves in such a manner that the trajectory of a point on \mathcal{S} may be that of a period- 2^n orbit, but the continuity of \mathcal{S} is maintained throughout the evolution.

To make the nature of this deformation of \mathcal{S} clear, consider Fig. 3 which shows $\mathcal{S} = \{\mathbf{c}(r, \theta, t) : 0 \leq \theta \leq 2\pi, r = 0.219, t\}$ for $t = t_1, t_2, t_3, t_4$ where r is measured in the fractions of the system size. For $r = 0.219$ and almost all θ the local attractor is a period-2 limit cycle (P-2) with a small inner loop and a large outer loop. For reference, one period of P-2 is shown in each panel of Fig. 3 as a light solid line. The filled diamonds are points on \mathcal{S} . One sees that at any fixed time instant, $t = t_i$, \mathcal{S} is a simple closed curve in the \mathbf{c} phase space. This curve deforms as time progresses as follows: In 3(a) \mathcal{S} is a large closed curve that lies on the outer loop of P-2. As time increases (b) \mathcal{S} deforms so that its upper left portion lies on the inner loop of P-2 and smoothly joins to that portion of \mathcal{S} remaining on the outer loop. In panel (c) at time t_3 one sees that deformation is complete and \mathcal{S} lies entirely along the inner loop of P-2. Finally, in (d), \mathcal{S} expands so that when the expansion is complete it again lies along the outer loop of P-2 as in panel (a). Analogous but more complicated versions of such deformations are seen for higher periodic orbits.

We have observed above that in the course of the dynamics the curve \mathcal{S} joins portions of the inner and outer loops of the P-2 attractor (panel (c) in Fig. 3). In view of the continuity of the medium, this implies that there must be a point on a circle with $r = r'$ where the period-2 bands merge and the dynamics becomes effectively period-1. This accounts for the above-mentioned broken circular symmetry and the fact that the period-doubling progression observed along rays may exhibit different characteristics due to band merging at certain angles θ .

As one moves from the vicinity of a defect to the bulk medium the nature of the spatiotemporal dynamics may be summarized as follows: Close to the defect the local dynamics is approximately periodic and as r increases a critical value of r is reached where the local dynamics undergoes a “bifurcation” to period-2. This process continues until a chaotic attractor is obtained. As in noisy maps and flows this spatial period-doubling sequence truncates at some finite value beyond which a noisy chaotic attractor is found. The number of noisy period doublings that may be observed is a function of the system parameters, for example the diffusion coefficient, and the characteristic distance between defects or between a defect and the boundaries.

The phenomena described here should exist in any system exhibiting a period-doubling sequence to chaos and be experimentally observable, for example, in chemical reactions carried out in continuously-fed unstirred reactors. [12] If conditions are adjusted so that the spatially-homogeneous system supports a chaotic attractor, well known in the Belousov-Zhabotinsky reaction [13], then suitable initial conditions, similar to those that are commonly used to initiate spiral waves in excitable media, should produce the spiral wave states described here. Typically, in experiments on well-stirred systems, the period doubling sequence is often difficult to resolve since it occurs in a very narrow parameter range. This does not imply that the period doubling that occurs as one moves away from the defect is confined to a narrow spatial domain. To observe the phenomena described in this paper it is only necessary to place the system in the chaotic regime, or near it. The spiral structure will locally organize the dynamics and the passage to the chaotic dynamics far from the defect should be observable.

The work suggests the possibility of a variety of phenomena whose existence depends on at least three phase space variables. Questions concerning the nature of defect dynamics and interactions in chaotic media remain to be explored.

This work was supported in part by a grant from the Natural Sciences and Engineering Research Council of Canada and by a Killam Research Fellowship (R.K.).

[1] A.S. Mikhailov, *Foundations of Synergetics I. Distributed Active Systems*, (Springer-Verlag, Berlin, 1994); *Chemical Waves and Patterns*, eds. R. Kapral and K. Showalter, (Kluwer, Dordrecht, 1995).

- [2] P. Coullet, L. Gil and J. Lega, Phys. Rev. Lett. **62**, 161 (1989); Physica D **37**, 91 (1989).
- [3] N.D. Mermin, Rev. Mod. Phys. **51**, 591 (1979).
- [4] K.-D. Willamowski and O.E. Rössler, Z. Naturforsch. **35a**, 317 (1980).
- [5] X.-G. Wu and R. Kapral, J. Chem. Phys. **100**, 5936 (1994).
- [6] One may also use a spherical polar coordinate system centered on \mathbf{c}^* in which case the azimuthal angle can be used to define the phase.
- [7] The simulations were carried out using both explicit Euler methods with time and space steps of $\Delta t = 10^{-3} - 10^{-4}$ and $\Delta x = 10^{-2} - 2 \times 10^{-3}$, respectively, as well as split-step Fourier transform methods for periodic and no-flux boundary conditions.
- [8] Initial conditions were chosen to favor the formation of a topological defect. The $c_x(\mathbf{r})$ and $c_y(\mathbf{r})$ concentrations were varied to produce spatially orthogonal gradients while the c_z concentration was fixed at $c_z(\mathbf{r}) = c_z^*$, so that a defect was introduced in the center of the spatial domain. It is possible to choose smoothly varying phase conditions so no defects form; thus, the defect-mediated turbulent state coexists with simple phase turbulence.
- [9] Such behavior is seen in coupled map lattices with chaotic elements [L. Brunnet, H. Chaté and P. Manneville, Physica D, **78**, 141 (1994).]
- [10] In the spatially-distributed medium the local dynamics is always perturbed by its neighborhood. We use the term “perturbed” period- 2^n or chaotic orbit to denote local attractor whose phase space probability density is highly peaked along the corresponding period- 2^n or chaotic attractor. Henceforth, all periodic or chaotic attractors are to be understood in this sense, even if the adjective “perturbed” is omitted.
- [11] J.P. Crutchfield, J.D. Farmer and B.A. Huberman, Phys. Rep. **92**, 45 (1982).
- [12] G.S. Skinner and H.L. Swinney, Physica D **48**, 1 (1991).
- [13] F. Argoul, A. Arneodo, P. Richetti, J.C. Roux and H.L. Swinney, Acc. Chem. Res. **20**, 436 (1987).

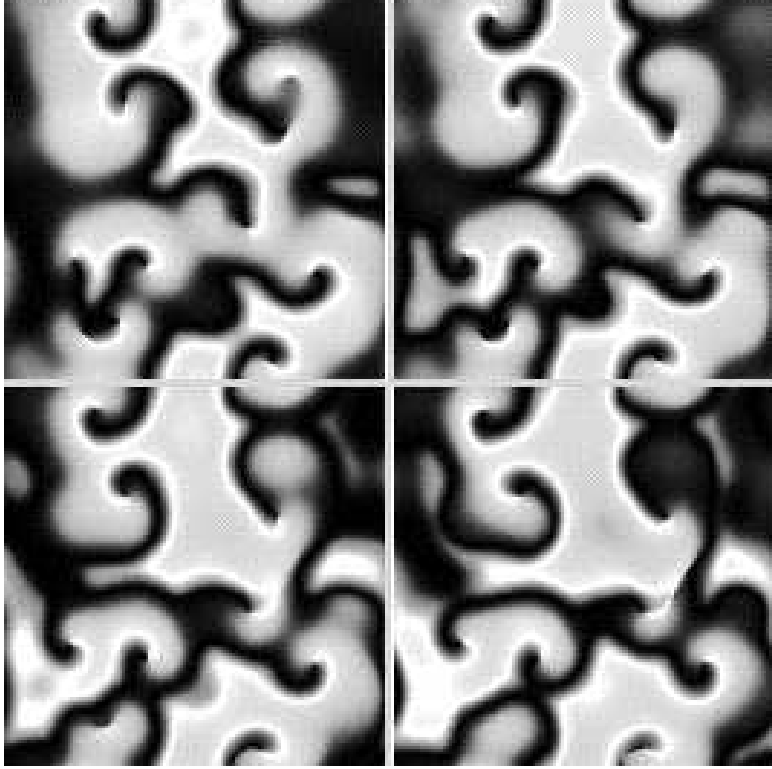


FIG. 1. Defect-mediated turbulence in a chaotic medium. The local phase $\phi(x, y, t)$ is shown as gray shades in the spatial xy plane. Defects can be located as the termini of the white, equiphase contour lines. The time interval between frames corresponds to one period of the spiral rotation. Time increases from left to right and top to bottom. Rate parameters are: $\kappa_1 = 31.2$, $\kappa_{-1} = 0.2$, $\kappa_2 = 1.572$, $\kappa_{-2} = 0.1$, $\kappa_3 = 10.8$, $\kappa_{-3} = 0.12$, $\kappa_4 = 1.02$, $\kappa_{-4} = 0.01$, $\kappa_5 = 16.5$, $\kappa_{-5} = 0.5$. The integration time step is $\Delta t = 5 \times 10^{-4}$ and the scaled diffusion coefficient is $D\Delta t/(\Delta x)^2 = 10^{-3}$. Periodic boundary conditions are used.

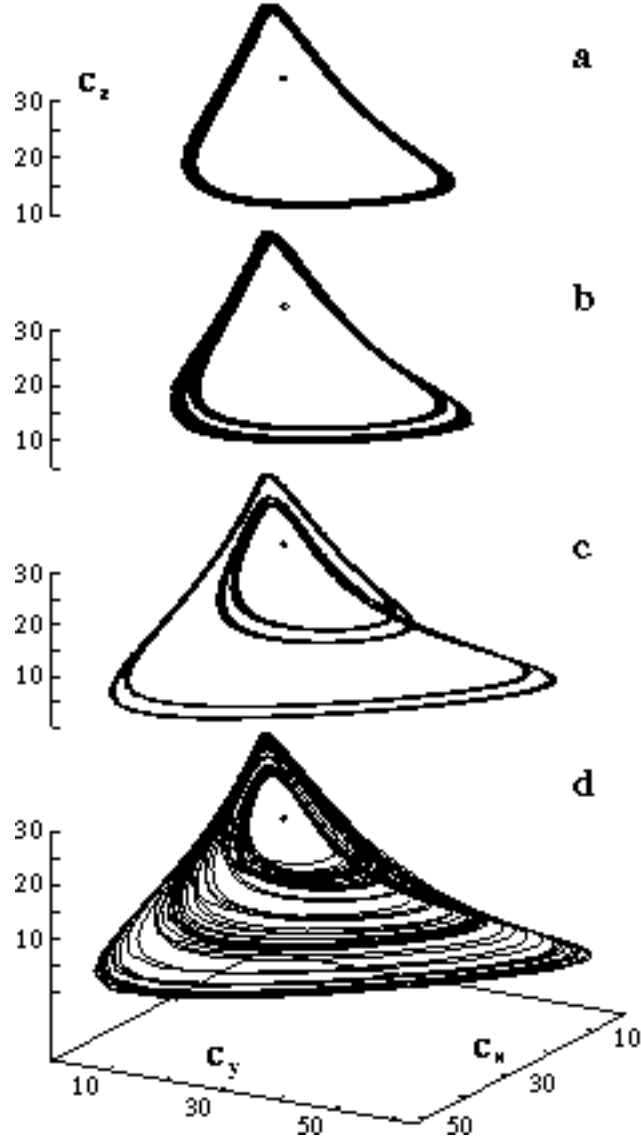


FIG. 2. Phase space trajectories $\mathbf{c}(r, \theta, t)$ for $\kappa_2 = 1.567$ and the other rate parameters as in Fig. 1 at fixed $\theta = 3/4\pi$ for three values of r : (a) period-1 limit cycle at $r = 0.194$; (b) period-2 orbit at $r = 0.206$ and (c) period-4 orbit at $r = 0.344$. The scaled diffusion coefficient is $D\Delta t/(\Delta x)^2 = 0.01$ and no-flux boundary conditions are used. (d) Local chaotic dynamics at a point in Fig. 1 far removed from a defect.

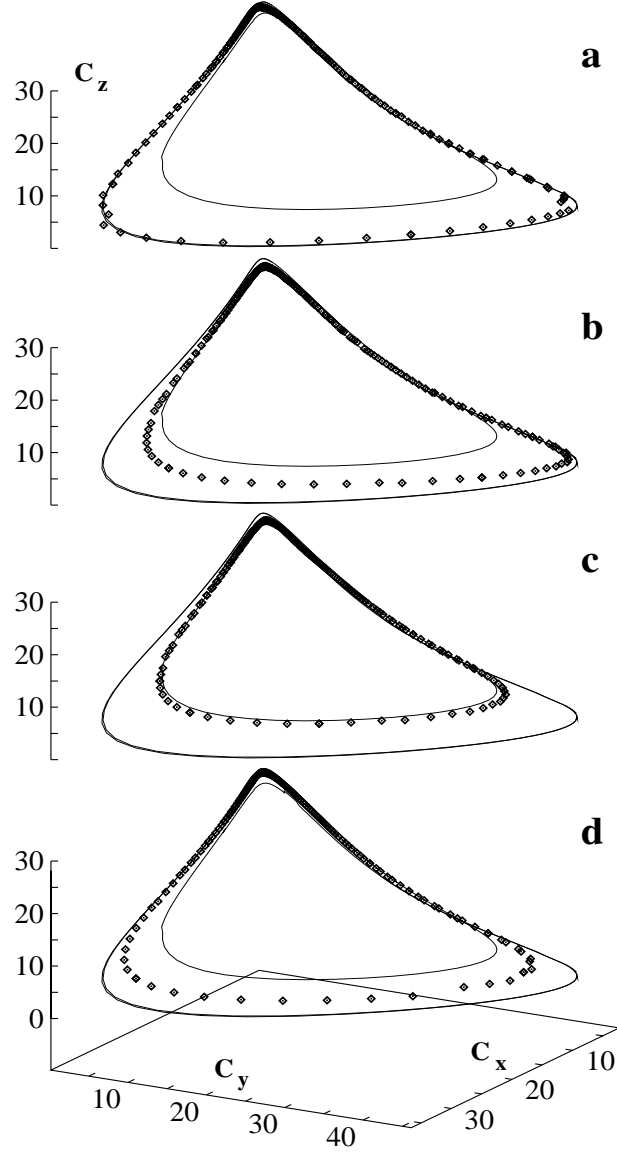


FIG. 3. Plots of \mathcal{S} in the \mathbf{c} phase space for $r = 0.219$ for four different times t_i : (a) $t_1 = 0.0$; (b) $t_2 = 0.209$; (c) $t_3 = 0.326$ and (d) $t_4 = 0.721$; time is expressed in the fractions of average time period of P-2. \mathcal{S} is shown as filled diamonds while the solid curve represents one period of the P-2 orbit at $(r = 0.219, \theta = 3/4\pi)$. The simulation conditions are the same as in Fig. 2.